KFKI-1981-44

J. GAZSÓ

DETERMINATION OF THE DENSITY
OF THE LOCALIZED STATES FROM
THE FIELD EFFECT IN WIDE GAP SEMICONDUCTORS

Hungarian Academy of Sciences

CENTRAL
RESEARCH
INSTITUTE FOR
PHYSICS

BUDAPEST

DETERMINATION OF THE DENSITY OF THE LOCALIZED STATES FROM THE FIELD EFFECT IN WIDE GAP SEMICONDUCTORS

J. Gazsó

Central Research Institute for Physics
H-1525 Budapest 114, P.O.B. 49, Hungary

ABSTRACT

The paper presents an analysis of the problem how the density of the localized states g_{LOC} can be deduced from field effect data. A simple model is adopted with g_{LOC} = constant in energy and in space. Precise computer solutions serve as data; approximate procedures generalize the findings and emphasize the essentials. Explicit formulas are derived which enable the direct calculation of g_{LOC} from data. In addition, a new possibility is pointed out how the trap-free value of the mobility may be measured even in the presence of deep traps.

АННОТАЦИЯ

Работа посвящена анализу проблемы определения плотности локализованных состояний ($g_{лок}$) из данных эффекта поля. Обычная модель адаптирована при помощи выбора определенной плотности состояний $g_{лок}$ = const, которая является постоянной в пространстве и энергии. Из теоретической модели с помощью вычислительной машины получено точное решение - семейство кривых. Обсуждаемое в статье решение с помощью приближенных аналитических методов выражает зависимость между параметрами модели и обобщает решение проблемы. Определены явные выражения, позволяющие вычислить $g_{лок}$ непосредственно из данных. В дальнейшем указано на новую возможность измерения подвижности, свободной от влияния ловушек.

KIVONAT

Megvizsgáljuk, hogy miként határozható meg a g_{LOC} lokalizált állapotsürüség a tér-effektus adataiból. Evégett tanulmányozzuk egy modell (g_{LOC} = kontans térben és energiában) elméleti viselkedését. Explicit képleteket vezetünk le a g_{LOC} közvetlen kiszámitására. Rámutatunk egy uj lehetőségre, amely szerint a mozgékonyság csapdamentes értékét a mély csapdák jelenlétében is meg lehet határozni.

INTRODUCTION

The term "field effect" is associated with changes in the conductance of a piece of semiconductor under the influence of a capacitively applied electric field perpendicular to the direction of the conductance considered. Since the operational principles appear so simple it is tempting to think of the possibilities to make use of this technique for the exploration of the electronic properties of the semiconductor. We are interested in wide gap ($E_g \geq 1$ eV) semiconductors such that the forbidden zone contains a sufficient density of localized states g_{LOC} ($\geq 10^{15}$ cm^{-3}eV^{-1}), distributed broadly in energy over the gap. Wide gap amorphous semiconductors are agreed to embody these features [1]. Indeed, amorphous silicon prepared by the glow discharge method was the subject of the pioneering work to apply the field effect for the determination of g_{LOC} [2]. Although several papers have been published on this topic, the present author is convinced that there is still room for precise model calculations. All the more so since there is a need for formulas based on careful studies so that any researcher inexperienced as yet in this type of evaluation should be able to make use of them in his attempts to interpret experimental findings without himself getting involved in the details of the numerical analysis.

Our strategy is to proceed from simple to more elaborate models of gap states and to examine in each case how the features of the band diagram are reflected in the observable quantities. Particular attention will be paid to develop procedures by which the opposite task, i.e. the fitting of a model to experimental data can be carried out. The present paper is but the first of an intended series and it will be restricted to the simplest model: to a thin film of a wide gap semiconductor with negligible surface states, containing acceptor and donor states dis-

tributed uniformly in energy over the gap, the system being in thermal equilibrium at not too low temperatures (T > 100 K) and conductance being due to mobile carriers in the conduction and the valence bands. We adopted a twofold procedure: First, computer solutions were generated, using everywhere the fomulas encountered later in this paper in their more precise forms. Second, in order to understand the significance of the results and to convey a feel for the problem, a parallel procedure of more approximate nature was developed and is described in this paper.

Description of the model

To simplify the treatment, as much symmetry as possible will be built into our model. In Fig. 1 is seen a thin strip of a semiconductor film GHMLPQRS, prepared in planar gap-type configuration, where the two metal contacts ("source" and "drain") are represented by EFGH and JKLM. Our attention will be focussed onto the central piece of the semiconductor marked by $ABCDA'B'C'D'$. The system of spatial coordinates is positioned at the centre so that the axes x, y and z are parallel to $A'A$, AB and CB.

The thickness of the semiconductor film $d = AA'$ is of the order of 1 micron, while AD = AB are greater by at least an order of magnitude. (The assumption AD = AB is merely because we want to make use of the notion "square conductance" in (6)). The faces $ABB'A'$ and $DCC'D'$ are imaginary: the purpose of their introduction is to set apart the edge regions where the physical conditions deviate from those inside $ABCDA'B'C'D'$. They are supposed to be displaced from the respective edges EF and JK by about d.

The external electric field modulating the conductance acts in the

x direction. To be more precise, the important quantity which is continuous upon crossing the boundaries ABCD and A'B'C'D' is D, the x component of the dielectric displacement vector at $|x| = d/2$:

$$D = \varepsilon_o \varepsilon_2 F_s = \varepsilon_o F_o \tag{1}$$

where $\varepsilon_o = 8.8542 \cdot 10^{-14}$ A$\cdot$s$\cdot$V$^{-1}\cdot$cm^{-1} is the vacumm permittivity, ε_2 is the relative permittivity of the semiconductor ($\varepsilon_2 = 12$ is taken in numerical examples), and

$$F_s = \lim_{\delta \to +o} F(|x| = d/2-\delta) \tag{2}$$

is the surface field strength in the semiconductor, and F_o is the equivalent vacuum field strength; $F_{o,max} \doteq 1.2 \cdot 10^6$ V/cm was chosen arbitrarily. (Of course, the establishment of D in practice requires insulator spacers and gate electrodes, not shown in Fig. 1.) It is assumed further that the condition of homogeneity in D

$$\frac{\partial D}{\partial y} = \frac{\partial D}{\partial z} = 0 \tag{3}$$

is fulfilled along ABCD and A'B'C'D' to a reasonable degree; the problem is thus reduced to the single dimension of x.

The steady state of the model system can be described fully by the electric potential $\phi(x)$. Obviously $\phi(x)$ must obey the boundary conditions:

$$\lim_{\delta \to +O} \frac{d\phi}{dx}\bigg|_{|x| = d/2-\delta} = -F_s = -F_o/\varepsilon_2 \tag{4}$$

and must be a solution to the Poisson equation:

$$-\varepsilon_o \varepsilon_2 \cdot \frac{d^2 \emptyset(x, g_{LOC}, F_o, \text{PARAMETERS})}{dx^2} = \rho(\emptyset(x, g_{LOC}, F_o, \text{PARAMETERS})) \qquad (5)$$

In (5) we have chosen the form of the argument lists deliberately in order to emphasize the mutual dependences of $\emptyset$ and ρ on each other. g_{LOC} and F_o are promoted from the rest of variables due to their importances. The denomination PARAMETERS is a group name for such parameters as T, d, E_g and the effective masses m_e and m_h.

The square conductance G_z of the slab ABCDA'B'C'D' in the z direction will be, as a rule, of the form

$$G_z(g_{LOC}, F_o, \text{PARAMETERS}) = \int_{-d/2}^{d/2} \sigma(\emptyset(x, g_{LOC}, F_o, \text{PARAMETERS}))dx \qquad (6)$$

where σ represents the (local) conductivity. The desired end is the knowledge of G_z in dependence on its arguments, since then an experimental G_z versus F_o relationship could, in principle, be used for the determination of g_{LOC}. We admit that the rather involved nature of equations (4)-(6) may appear to be dissuasive at this stage, not to mention the further difficulty that G_z is not equivalent automatically to the conductance G_{SD} between EFGH and JKLM.

(One might be led first to believe that should it be possible to make contacts directly to ABB'A' and DCC'D', this latter difficulty would be eliminated. Then, however, ABB'A' and DCC'D' would have to become equipotentials themselves, which surely would destroy the symmetries leading to the one-dimensional treatment.) Further remarks on the amenability of G_z will be among the conclusions following eq.(38).

Our model semiconductor has parabolic conduction and valence bands with effective masses equal to that of the free electron. Localized acceptor and donor states are distributed homogeneously in space and uniformly in energy over the gap:

$$g_A = g_D = g_{LOC}/2 \tag{7}$$

g_{LOC} was varied in computer simulation in the range of $10^{15} cm^{-3} eV^{-1}$ to $10^{19} cm^{-3} eV^{-1}$ by 0.2 steps in the decimal exponent. Surface states may be present only in negligible amounts compared to the dominant charge supplying states. Not too low temperatures (e.g. 195 K and 295 K) are considered.

Such a structure if left in thermal equilibrium and in zero electric field would possess not only zero overall charge but as a consequence of the symmetries local charge neutrality would prevail everywhere. Hence the electron energy diagram is horizontal, and the Fermi-level coincides with the medial line of the gap. The band edges are at $E_c = E_g/2$ and $E_v = -E_g/2$, respectively. ($E_g = 1.6$ eV in numerical examples.) This zero-field position will be the reference in our discussion.

If a non-zero external field is switched onto this structure and is left there for a time long enough so that a new steady state may be reached by the rearrangement of the internal charges (no carriers may cross the boundaries ABCD and A'B'C'D'), then a distorted band diagram will result as shown schematically in Fig. 2. Since no current flows in the x direction, the Fermi level has kept its previous horizontal position. It will be useful to denote by U(x) the difference

$$U(x) = (\text{Midgap energy at } x) - (\text{Fermi-level}) \tag{8}$$

and to introduce its dimensionless counterpart u(x) by

$$U(x) = u(x) \cdot kT \tag{9}$$

where $k = 8.617 \cdot 10^{-5}$ eV/K is Boltzmann constant. The relation of U and u to the electric potential $\emptyset$ is:

$$-\emptyset(x) = \frac{U(x)}{q^*} = \frac{kT}{q^*} u(x) \tag{10}$$

If $\emptyset$ and U are to be measured in [volts] and [electronvolts], respectively, then q^* is of the units [electronvolts/volts], and has the numerical value 1. The latter fact justifies its distinction from the elementary charge $q = 1.6022 \cdot 10^{19}$ A·s.

The charge density ρ_{LOC}

Let us first express the charge contribution from the occupied acceptor states:

$$\rho_A(U(x)) = -q \cdot \int_{-\frac{E_g}{2}+U(x)}^{\frac{E_g}{2}+U(x)} g_A \cdot kT \cdot \frac{1}{1 + \exp(\frac{E}{kT})} \cdot \frac{dE}{kT} = -qg_A \cdot [E_g - kT\ln \frac{1+\exp(\frac{E_g}{2kT} + u)}{1+\exp(u - \frac{E_g}{2kT})}] \tag{11}$$

Empty donors give a charge contribution in an analogue way:

$$\rho_D(U(x)) = q \cdot \int_{-\frac{E_g}{2}+U(x)}^{\frac{E_g}{2}+U(x)} g_D \cdot kT \cdot (1 - \frac{1}{1 + \exp(\frac{E}{kT})}) \cdot \frac{dE}{kT} = qg_D kT\ln \frac{1 + \exp(\frac{E_g}{2kT} + u)}{1 + \exp(u - \frac{E_g}{2kT})} \tag{12}$$

Then, by taking use of (11),(12) and (7):

$$\rho_{LOC}(u(x)) = g_{LOC} \cdot kT \cdot q \cdot [\ln \frac{1 + \exp(\frac{E_g}{2kT} + u)}{1 + \exp(u - \frac{E_g}{2kT})} - \frac{E_g}{2kT}] \qquad (13)$$

It will be sufficient to restrict ourselves to the study of $\rho_{LOC}(u)$ for $u \geq 0$ only, since from (13):

$$\rho_{LOC}(u) = - \rho_{LOC}(-u). \qquad (14)$$

Typical orders of magnitudes are e.g. at $T = 295$ K: $\frac{E_g}{2kT} \approx 31.5$ and $\exp(- \frac{E_g}{2kT}) \sim 2 \cdot 10^{-14}$. By this:

$$\rho_{LOC}(u(x)) \simeq q \cdot g_{LOC} \cdot kT \cdot [u - \ln(1 + \exp(u - \frac{E_g}{2kT}))]. \qquad (15)$$

As long as the induced potential shift remains limited from above by

$$u(x) < \frac{E_g}{2kT} - 2 \qquad (16)$$

eq.(15) can be simplified further:

$$\rho_{LOC}(u(x)) \approx q \cdot g_{LOC} \cdot kT \cdot u(x) \qquad (17)$$

The simple form of (17) was one of the chief reasons to select the type of localized states distribution described in the preceding section. Computer solutions based on the more precise (15) form confirmed the validity of (16) for all practical circumstances.

Note in particular that the simple form of (17) is not a consequence of the Fermi-function being replaced by a step-function, even though that is frequently claimed for.

Mobile carriers

The delocalized carriers are important in two respects. First, the conductance G_z is by them. Second, one has to know the limits below which their share in the charge density becomes negligible since it is then that a reliable estimate on g_{LOC} may be hoped for.

For electrons, the function of the density of states is [3]:

$$g(E)dE = 4\pi \cdot \left(\frac{2m}{h^2}\right)^{3/2} \cdot (E-E_c)^{1/2} \cdot dE \tag{18}$$

By this, the electron concentration at x where the potential energy is displaced by U(x):

$$n(x) = \int_{\frac{E_g}{2} + U(x)}^{\infty} \frac{g(E)dE}{1+\exp\left(\frac{E}{kT}\right)} = N_c \cdot \mathcal{F}_{1/2}\left(-\frac{E_g}{2kT} - u(x)\right) \tag{19}$$

Here [4]
$$N_c = 2 \cdot \left(\frac{2\pi mkT}{h^2}\right)^{3/2} \tag{20}$$

and $\mathcal{F}_{1/2}(\eta)$ is a member of the more general set of Fermi-Dirac integrals [5]:

$$\mathcal{F}_j(\eta) = \frac{1}{\Gamma(j+1)} \int_0^{\infty} \frac{y^j dy}{1+\exp(y-\eta)} \tag{21}$$

where $\Gamma(j+1)$ represents the gamma function [6]. It is of particular interest to us that for $\eta \geq 0$ $\mathcal{F}_j(\eta)$ can be expressed in a series expansion [6]:

$$\mathcal{F}_j(\eta) = \sum_{k=1}^{\infty} \frac{(-1)^{k+1}\exp(k\eta)}{k^{j+1}} \tag{22}$$

Thus for potential modulations not approaching $\frac{E_g}{2kT}$ simple expressions result:

$$n(x) \approx n_o e^{-u(x)} \tag{23}$$

$$p(x) \approx n_o e^{u(x)} \tag{24}$$

$$\rho_{DELOC}(x) \approx 2qn_o \cdot \sinh(u) \tag{25}$$

In (24)-(25), the expressions for holes were taken by analogy, and

$$n_o = N_c \cdot \exp\left(-\frac{E_g}{2kT}\right) \tag{26}$$

stands for the intrinsic concentration.

With the help of (17) and (25), eq.(5) can be rewritten:

$$\frac{\varepsilon_o \varepsilon_2}{q} \frac{kT}{q^*} \frac{d^2 u(x)}{dx^2} = g_{LOC} \cdot kT \cdot u(x) + 2n_o \cdot \sinh(u(x)) \tag{27}$$

together with the boundary conditions from (4):

$$\varepsilon_2 \cdot \frac{kT}{q^*} \cdot u_s' = F_s \tag{28a}$$

where $\quad u_s' = \lim\limits_{\delta \to +o} \frac{du}{dx}\bigg|_{|x| = d/2-\delta}$ $\tag{28b}$

The symmetry properties of the sought $u(x)$ in (27)-(28) reveal that it should be an odd function of x:

$$u(x) = -u(-x) \tag{29}$$

In particular,

$$u(x=o) = 0. \tag{30}$$

Then it will be enough to solve (27) with respect to (30) and to (28)

only for $0 \leq x \leq d/2$.

Conduction in delocalized bands

It is well established in solid state physics that the influence of different scattering mechanisms on the resulting drift mobility can be best described by a characteristic exponent r in the energetic dependence [7]. Thus the conductivity formulas for electrons and holes:

$$\sigma(u(x)) = q\mu_c \cdot \int_o^\infty \frac{y^{1/2+r} dy N_c \cdot \frac{2}{\sqrt{\pi}}}{1+\exp\left(y+u \pm \frac{E_g}{2kT}\right)} = q\mu_c \cdot N_c \cdot \frac{\Gamma(r+3/2)}{\Gamma(3/2)} \mathcal{F}_{r+1/2}\left(-u \mp \frac{E_g}{2kT}\right) \qquad (31)$$

where the upper sign stands for electrons, and μ_c is the mobility of carriers with kinetic energy kT. Accordingly $\mu_c \sim T^r$. The probable value for r is 3/2 when scattering is dominated by the numerous charged imperfections like in our proposed model. Now the (22) series expansion is applicable to (31), too. We want to point out that the exponent j+1 of k in the denominators of (22) will be about 3, thus reducing further the relative importance of higher terms. In other words: the plot of the $\log \mathcal{F}_2(\eta)$ as function of η (Fig. 3) is an even better straight line than $\log \mathcal{F}_{1/2}(\eta)$ vs. η, and the former resists degeneracy up to higher values of η.

The conclusion is that both conductivities can be safely used by retaining only the first terms:

$$\sigma_a(u(x)) = q \cdot \mu_{av} \cdot n_o \cdot e^{-u(x)} \qquad (32)$$

$$\sigma_h(u(x)) = q \cdot \mu_{av} \cdot n_o \cdot e^{u(x)} \qquad (33)$$

$$G_z = 2 \cdot \int_o^{d/2} (\sigma_e + \sigma_h) \cdot dx = 2 \cdot q \cdot \mu_A \cdot n_o \cdot \int_o^{d/2} \cosh(u(x)) \cdot dx \qquad (34)$$

where $\qquad \mu_{av} = \mu_c \cdot \frac{\Gamma(r+3/2)}{\Gamma(3/2)} \qquad\qquad (35)$

is the mobility averaged over a band.

Upper limit to the conductance increase

Before proceeding to solve Poisson equation and then evaluate the
(34) integral, we would like to demonstrate in a simple yet efficient
way how an upper limit can be set to the increase in G_z. We are con-
sidering cases when there are already more delocalized charges than
localized ones. If we denote by F_i the field at $x = 0$, and by $l=AB=BC$
the length of edges of the slab, them by Gauss law for $0 \leq x \leq d/2$:

$$l^2 \epsilon_o \epsilon_2 (F_s - F_i) = Q_{TOTAL} \simeq Q_{Majority} \approx q \cdot n_o \cdot \int_o^{d/2} \exp(u(x)) dx \qquad (36)$$

since the majority carriers are holes in the half-slab concerned for
$u(x) \geq 0$. At the same time the square conductance $G = G_z/2$ in the same
half of the slab is approximately:

$$G \approx q \cdot \mu_{av} \cdot n_o \cdot \int_o^{d/2} \exp(u(x)) dx \qquad (37)$$

Division of (37) by (36) yields then:

$$\frac{G}{l^2 \epsilon_o \epsilon_2 (F_s - F_i)} \approx \mu_{av} \qquad (38)$$

Obviously the maximum in G would be obtained for $F_i = 0$. As we shall see
in Fig. 4, whenever screening is by mobile carriers in films of about
1 micron thickness, then F_i remains at a fairly substantial proportion
of F_s. Nevertheless, we drew the dashed envelope curves in Figs 5-6 on
the assumptions that $F_i = 0$ and $l = 1$ cm. They demonstrate how easily the
ultimate limits to the conductance increase can be predicted. Note in
particular, that a number of parameters such as T, d, E_g or the effec-
tive masses, are absent in (38).

The most important lesson drawn from (38) and from the dashed lines in Figs 5-6 is for the interpretation of field-effect conductance measurements: that the slope of the logarithmic conductance plots may show a decrease with increasing surface field, and that this does not imply an increase in the density of the localized states.

Even some experimental application of (30) may not be entirely ruled out. It is tempting to think of the possibilities to determine μ_{av} directly with the help of (38): such a μ_{av} would be immune from the limitations imposed by the trapping/releasing processes known to operate in the presence of deep level traps, just because G is an equilibrium property. For this purpose, of course, G should be determined in such a way that the equilibrium, once achieved via rearrangement of charges in the x direction, should not be disturbed by either injection or depletion of the mobile carriers in the z direction (see Fig. 1); i.e. G should be measured by an appropriate small-signal AC method.

Solutions of Poisson equation when dominated by the localized charges

If we introduce

$$L = \left(\frac{\varepsilon_o \cdot \varepsilon_2}{q \cdot q^* \cdot g_{LOC}} \right)^{1/2} \tag{39}$$

and

$$L_i = \left(\frac{\varepsilon_o \cdot \varepsilon_2 \cdot kT}{2 \cdot q \cdot q^* \cdot n_o} \right)^{1/2} \tag{40}$$

as the so called Debye lengths due to the localized states and the mobile carriers, respectively, then (27) can be rewritten:

$$\frac{d^2 u}{dx^2} = \frac{u}{L^2} + \frac{sinh u}{L_i^2} \tag{41}$$

Typical magnitudes for L are displayed in Fig. 7. Note that L is independent of T. On the other hand L_i varies strongly with T, because n_o in the denominator of (30) is of activated type (see (26)): L_i = 1418.84 cm for T = 195 K and L_i = 0.4 cm for T = 295 K. Owing to the great difference in the magnitudes of L^2 and L_i^2, there will be a range for $0 \leq u \leq u_{cr}$ when the second, non-linear term in (41) may be neglected. The critical u_{cr} values are given by the solutions of the transcendental equation

$$\frac{u_{cr}}{L^2} = p \cdot \frac{\sinh u_{cr}}{L_i^2} \qquad (42)$$

and are shown in Fig. 8 for p = 0.01, 0.1 and 1. From this it is apparent that quite substantial modulations are allowed even for p = 0.01, and comparison with the precise computer results convinces that the neglect of the non-linear term will be felt in most cases only for p > 1.

The solution of the _linear_ second-order differential equation is

$$u(x) = \frac{u_s' \cdot L}{\cosh x_s/L} \cdot \sinh x/L \qquad (43)$$

where $x_s = d/2$. From this a further criterion

$$u_s' L \cdot \tanh x_s/L = u_s \leq u_{cr} \qquad (44)$$

may be developed. (44) sets upper limit to the inducing field strength; its dependence is plotted in Fig. 9. The quantity of $L \cdot \tanh\left(x_s/L\right)$ is seen of importance; plots of it are given in Fig. 7.

Now an appropriate expression for G_z in (34) have to be found.

If we denote the conductance <u>increase</u> by ΔG and

$$\sigma_o = q \cdot \mu_{av} \cdot 2 \cdot n_o \tag{45}$$

then
$$\Delta G = \sigma_o \cdot \int_o^{x_s} (\cosh u(x) - 1) \cdot dx \tag{46}$$

From (43)
$$\frac{dx}{L} = \frac{du}{\sqrt{u^2 + b^2}} \tag{47}$$

where
$$b = L \cdot \frac{u_s'}{\cosh x_s/L} \tag{48}$$

so
$$\Delta G = \sigma_o \cdot L \cdot \int_{u=o}^{u_s} \frac{\cosh u - 1}{\sqrt{u^2 + b^2}} \, du \tag{49}$$

The difficulty in evaluating (49) is connected with the possibilities of very wide variations in the value of b (see Fig. 10).

The method of the logarithmic slope

One possible way out of the difficulties is suggested by the general impression gained from the close inspection of Figs 5-6 that there exists a domain in g_{LOC} and F_o where the plots of the <u>logarithm</u> of G/μ_{av} against F_o are apparently straight lines with slopes characteristic of g_{LOC}. (Figures 5 and 6 themselves may immediately be used for the determination of g_{LOC} if the parameters of an actual experiment happen to agree with those of our numerical examples. We would like, however, to devise procedures whose applicability is more general.)

Since in the range concerned

$$\Delta G \gg G_o = \sigma_o \cdot d/2 \tag{50}$$

then $\qquad \log G = \log(\Delta G) + \log\left(1 + \dfrac{G_o}{\Delta G}\right) \approx \log(\Delta G) + \dfrac{G_o}{\Delta G}$ (51)

i.e. by (50) $\qquad\qquad \log G \approx \log \Delta G$ (52)

On the other hand, with the help of (44):

$$\frac{d\log G}{du_s'} \approx \frac{du_s}{du_s'} \cdot \frac{d\log\Delta G}{du_s} = L \cdot \tanh(x_s/L) \cdot \frac{1}{\Delta G} \cdot \frac{d\Delta G}{du_s}$$ (53)

Since by virtue of (49)

$$\frac{d\Delta G}{du_s} = \sigma_o L \cdot \frac{\cosh u_s - 1}{\sqrt{u_s^2 + b^2}}$$ (54)

then $\qquad \dfrac{1}{L}\dfrac{d\log G}{du_s'} \approx \dfrac{\cosh u_s}{\sqrt{u_s^2 + b^2}} \cdot \left(\int\limits_{n=o}^{u_s} \dfrac{\cosh u - 1}{\sqrt{u^2 + b^2}}\, du\right)^{-1/2} = R(u_s,b)$ (55)

Numerical experience shows that for $u_s > 8$ values (see Fig. 11), encountered in the regime of the present interest, $R(u_s,b)$ can be expressed approximately as

$$R(u_s,b) \approx \left[\sum_{k=o}^{5} k!\left(\frac{u_s}{u_s^2 + b^2}\right)^k\right]^{-1}$$ (56)

Fig. 12 shows the behaviour of the $R(u_s,b)$ function. Since the average value of $R(u_s,b)$ for $u_s > 20$ is about $R_{av} \approx 0.975$, it follows then from (55),(28a) and (4) that

$$\frac{1}{L} \cdot \frac{d\log G}{dF_o} \cdot \frac{\varepsilon_2 \cdot kT}{q^*} \approx R_{av}$$ (57)

Finally, with the help of (39):

$$g_{LOC} = \frac{\epsilon_o \epsilon_2}{qq^*} \frac{1}{L^2} \approx \frac{\epsilon_o \cdot q^*}{\epsilon_2 \cdot q} \cdot [\frac{R_{av}}{kT \cdot \frac{dlogG}{dF_o}}]^2 \qquad (58)$$

This is a most useful formula for the calculation of a mean density of the localized states from field effect measurements. It is interesting to point out that owing to the logarithmic derivative no knowledge of σ_o (or E_g) is required. In principle, the g_{LOC} values derived by (58) may be refined further in an iteration loop via (48),(56) and (58), as many times as desirable.

The method of finding a minimum (when g_{LOC} is large)

Aware of the limitations to the applicability of the method of the logarithmic slope, we would like to develop another equally useful procedure devoted particularly to densities $g_{LOC} > 10^{18} cm^{-3} eV^{-1}$. One possible way to attain this end starts with noticing that in this range the parameter b in eq.(48) and in Fig. 10 becomes negligibly small: $b^2 \approx 0$. Then the critical integral in (49) simplifies and since the series expansion of the integrand is absolute convergent, it can be integrated by terms:

$$\Delta G(u_s) = \sigma_o L \int_{u=0}^{u_s} \frac{\cosh u - 1}{u} du = \sigma_o \cdot L \cdot \sum_{k=1}^{\infty} \frac{u_s^{2k}}{2k \cdot (2k)!} \qquad (59)$$

The plot of this ΔG versus u_s relationship is a smooth, featureless function. The crucial point is the realization that ΔG divided by u_s^3, on the other hand, exhibits a minimum since then the first few terms in the new infinite sum

$$\frac{1}{4u_s} + \frac{u_s}{96} + \frac{u_s^3}{4320} + \cdots \qquad (60)$$

indicate clearly the existence of such a minimum for $u_s > 0$. Indeed, the function (see Fig. 13)

$$f(z) = \frac{1}{z} \cdot \sum_{k=1}^{\infty} \frac{z^{2k}}{2k \cdot (2k)!} \qquad (61)$$

has a minimum point at

$$z_{min} = 3.438447864 \qquad (62)$$

where $\qquad f(z_{min}) = 0.1195937066 \qquad (63)$

By finding, therefore, the minimum of $\frac{\Delta G}{F_o^3}$ on experimental data points, it can be expressed in terms of the characteristic Debye length L:

$$\min(\frac{\Delta G}{F_o^3}) = (\frac{Lq^*}{\epsilon_2 kT})^3 \cdot \min(\frac{\Delta G}{u_s^3}) = \sigma_o L^4 (\frac{q^*}{\epsilon_2 kT})^3 \cdot 0.12 \qquad (64)$$

From this, the final formula for g_{LOC} can be expressed with the help of (39):

$$g_{LOC} = \frac{\epsilon_o}{q} [\frac{0.12 \sigma_o q^*}{\epsilon_2 \cdot (kT)^3 \cdot \min(\frac{\Delta G}{F_o^3})}]^{1/2} \qquad (65)$$

We have found that the respective ranges of applicability of formulas (58) and (65) are overlapping. Thus they provide a means for checking accuracy. As regards our artificial data sets, the agreement between the two g_{LOC} values was in general better than 1 %.

REFERENCES

[1] Mott N.F. and Davis E.A., Electronic processes in non-crystalline materials, U.P., Oxford, 1971.

[2] Spear W.E. and Le Comber P.G., J.Non-Crystalline Solids 8-10 (1972) 727

[3] Blakemore J., Semiconductor Statistics, Pergamon, Oxford, 1962, p.45

[4] as [3], p.79

[5] as [3], p.346

[6] as [3], p.357

[7] Anselm A.I., Introduction to the theory of semiconductors (in German). Akademie-Verlag, Berlin, 1964, p.308
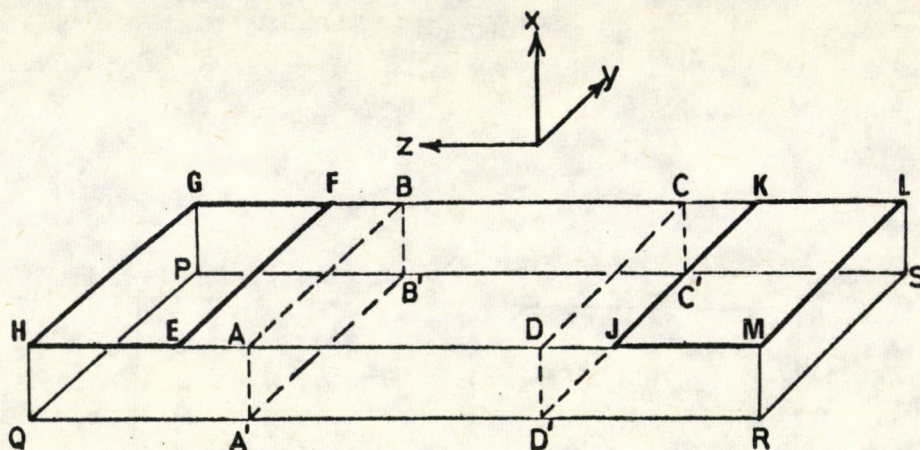
Fig. 1. Model geometry of the field effect
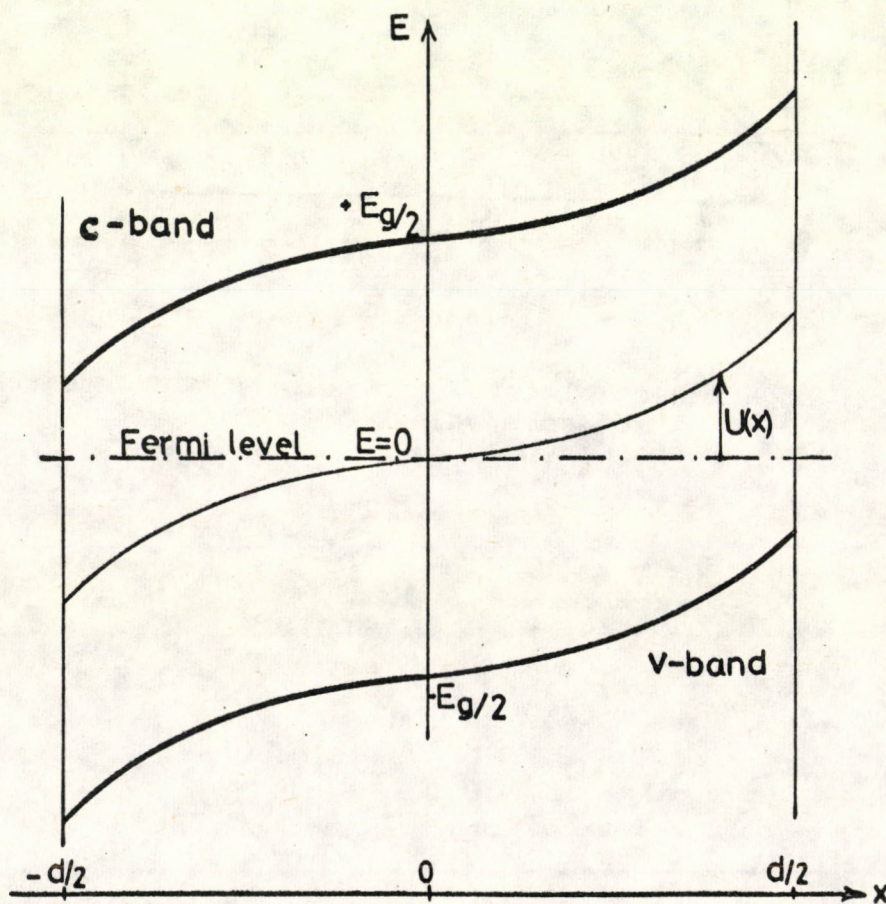
Fig. 2. Steady state band bending by the field effect
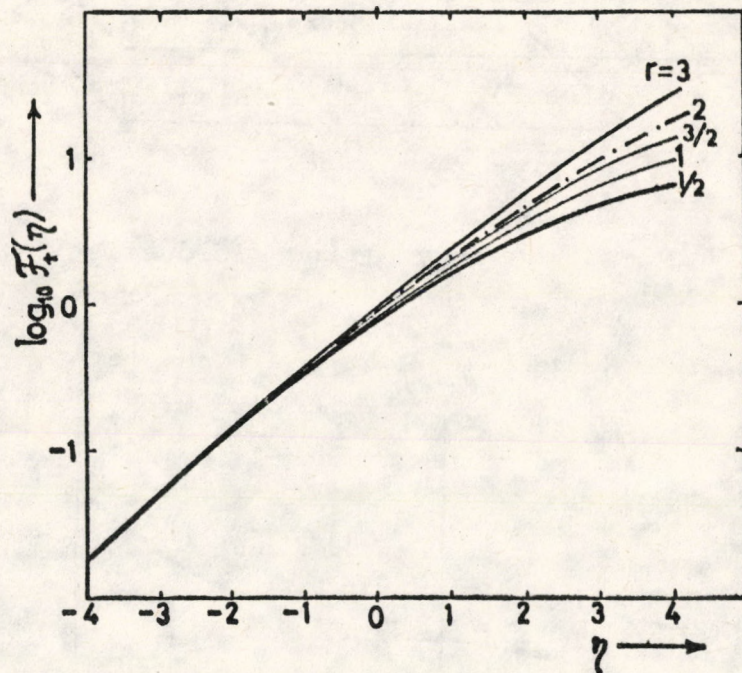
Fig. 3. Logarithmic plots of the Fermi-Dirac integrals
for some values of r
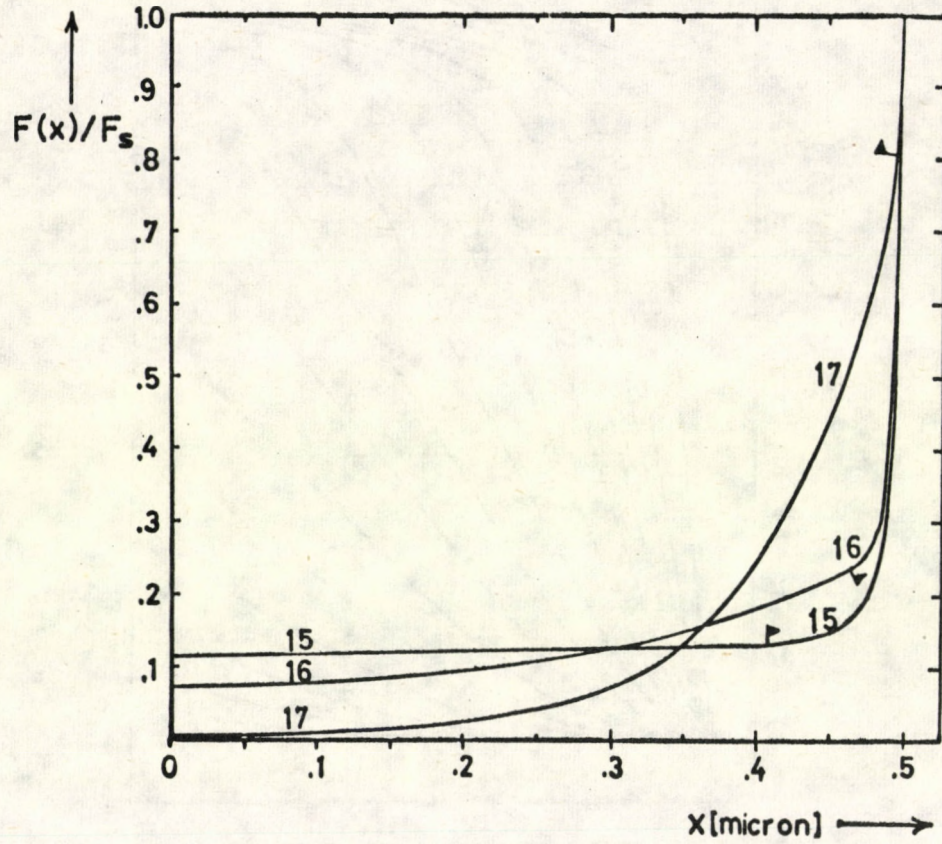
Fig. 4. Field screening effect along the half-thickness of the semiconductor film. The parameters are the decimal order of magnitude of g_{LOC} (in $[cm^{-3}eV^{-1}]$), and the flags indicate the approximate take-over by the mobile charges. ($F_s = 1.061 \cdot 10^5$ V/cm, T = 295 K)
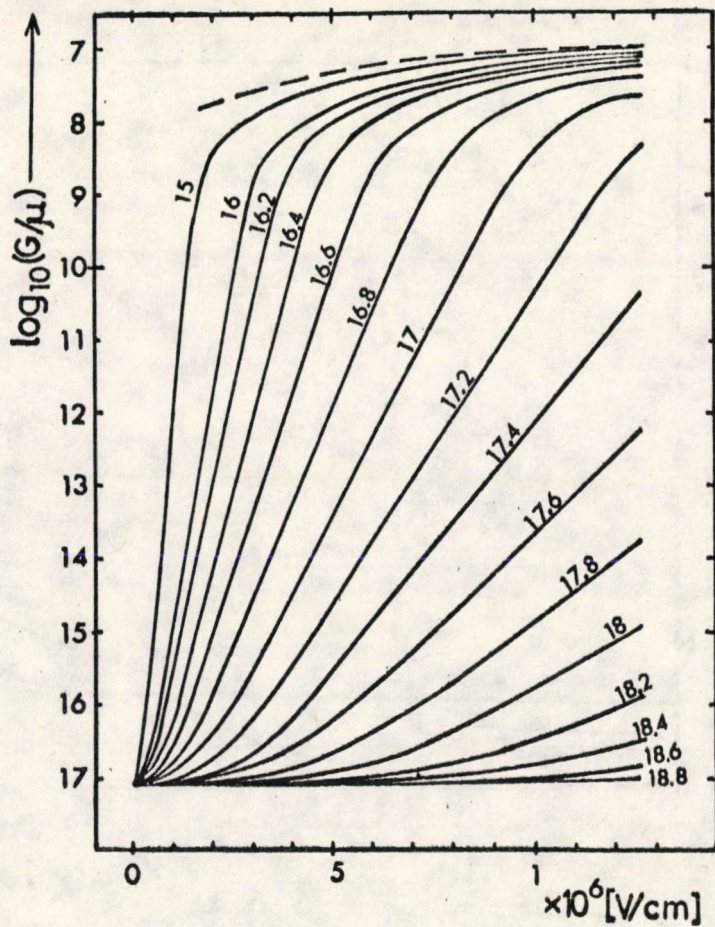
Fig. 5. Solid lines: Plots of log G/μ_{av} versus inducing field F_o.
Parameters are the orders of magnitude of
g_{LOC}. T = 295 K.
Dashed line: Envelope curve according to (38)
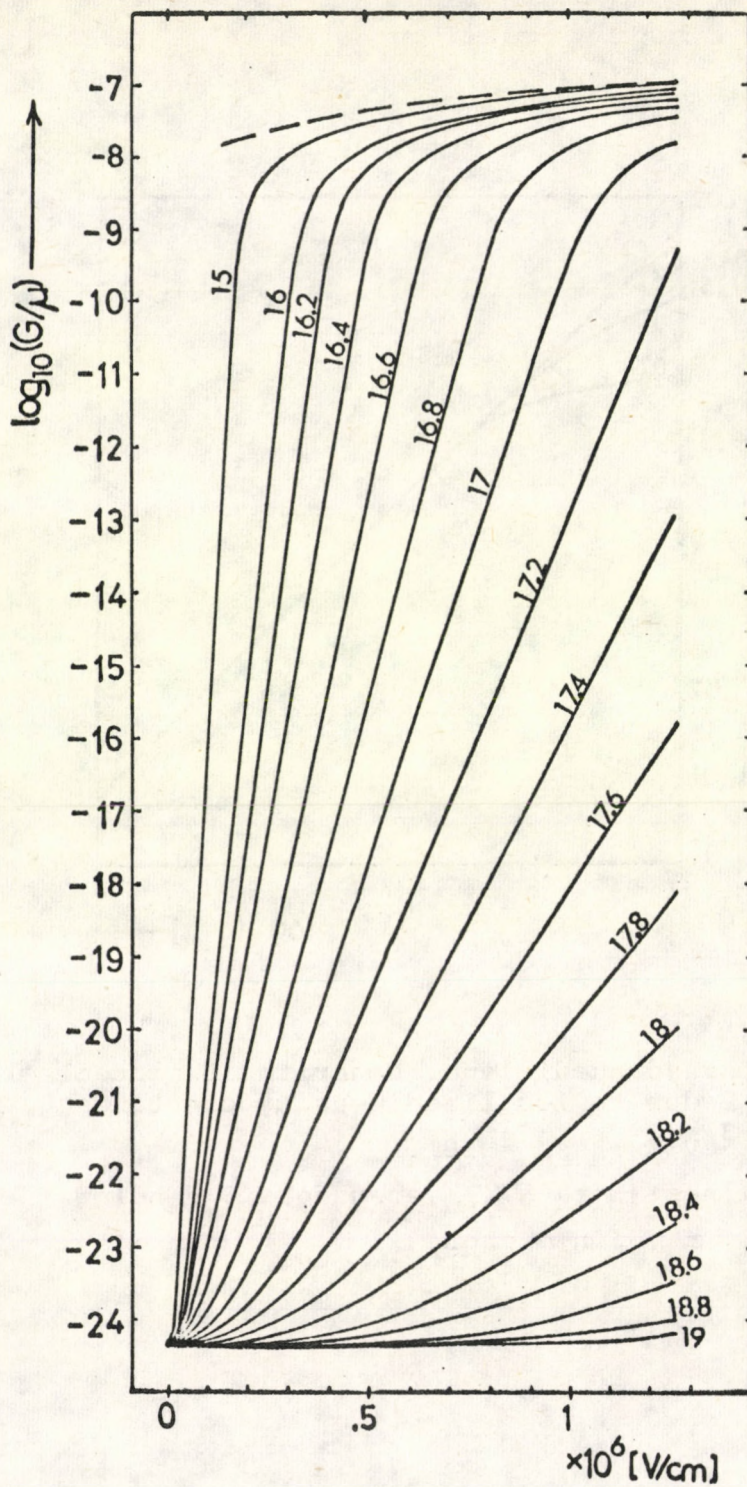
Fig. 6. As in Fig. 5, for T = 195 K
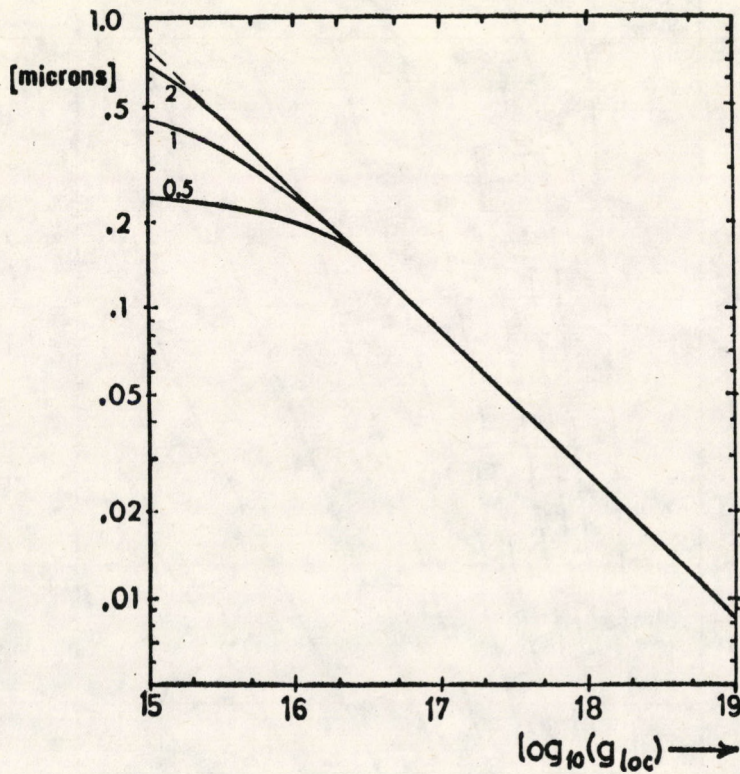
Fig. 7. Uppermost (dashed) line: Logarithmic plot of the Debye
length L due to localized density of states g_{LOC}
(in $[cm^{-3}eV^{-1}]$; $\varepsilon_2 = 12$).
Solid lines: $L \cdot \tanh \frac{d}{2L}$ versus g_{LOC}, d being the parameter
(in [microns]).
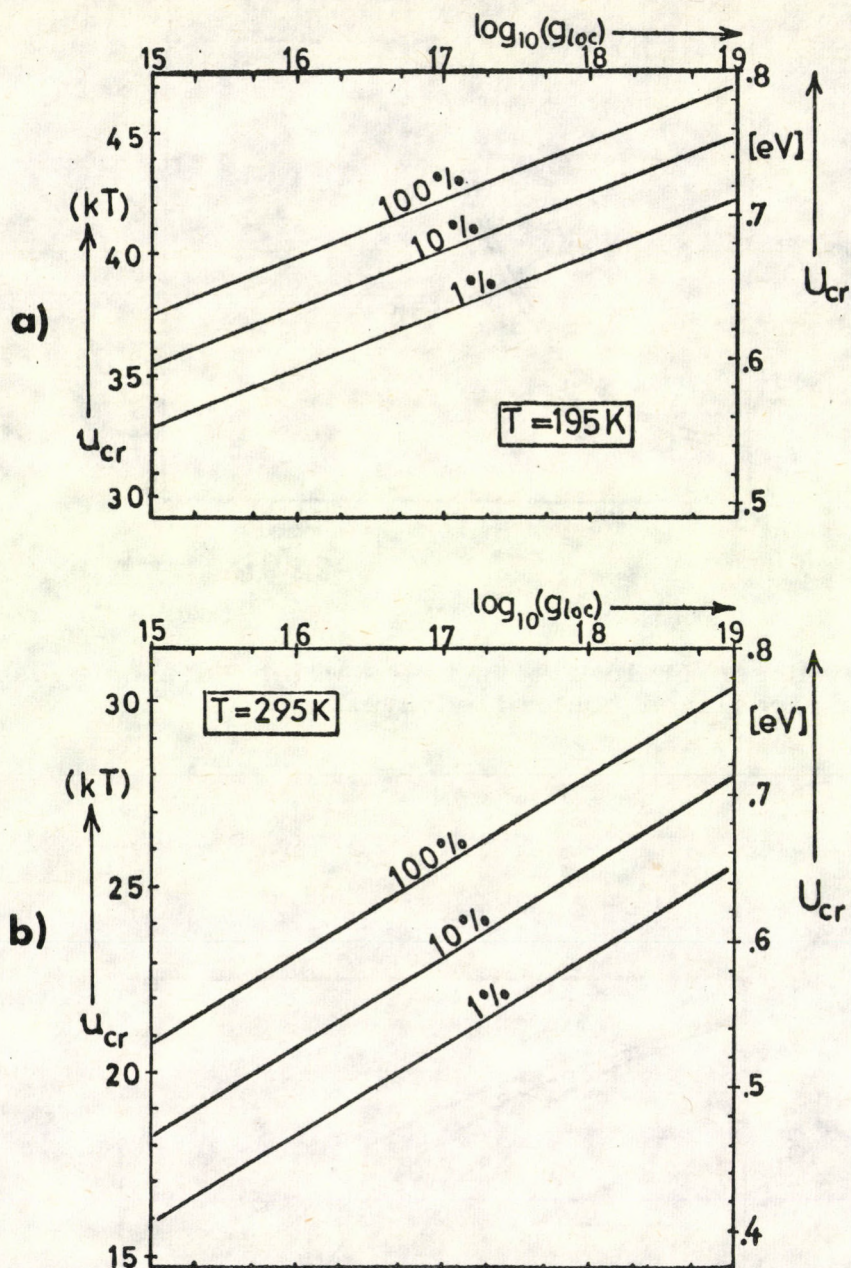
Fig. 8. The critical potential modulations where the charge
density from mobile carriers equals the indicated
proportion of that from g_{LOC}
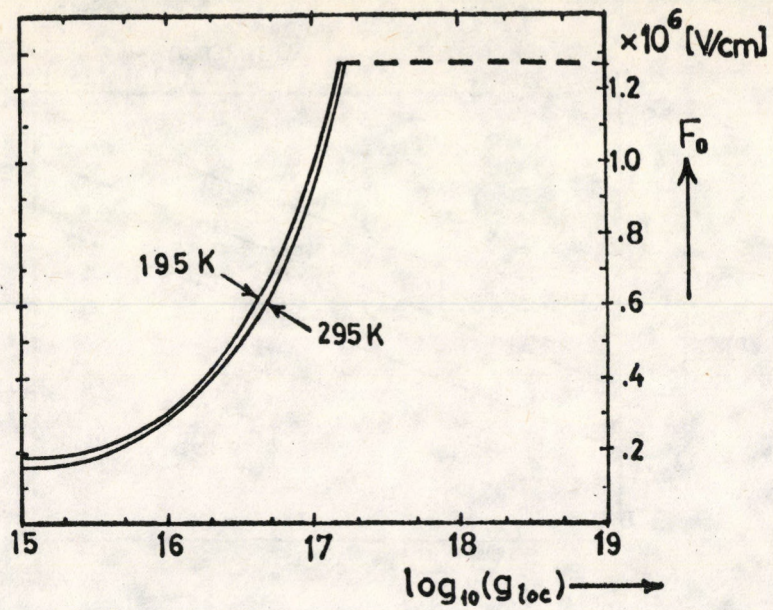
Fig. 9. Upper field limits below which Poisson equation is localized controlled everywhere
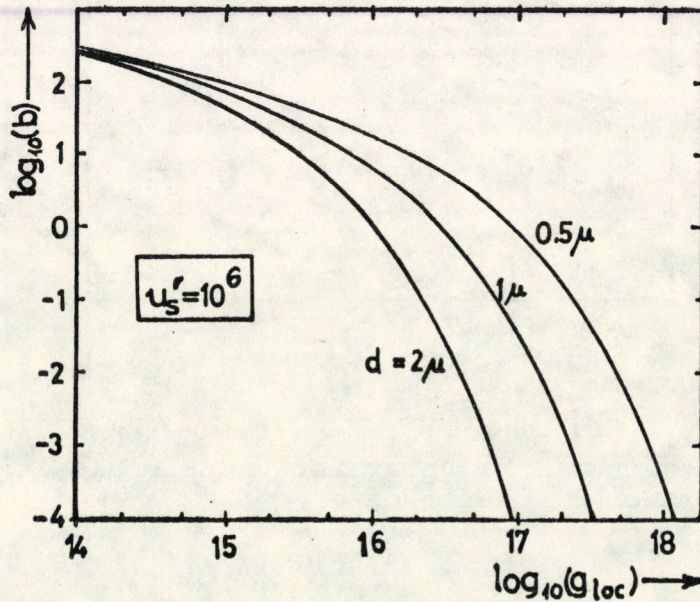
Fig. 10. Behaviour of the b values of eq.(48) against g_{LOC}
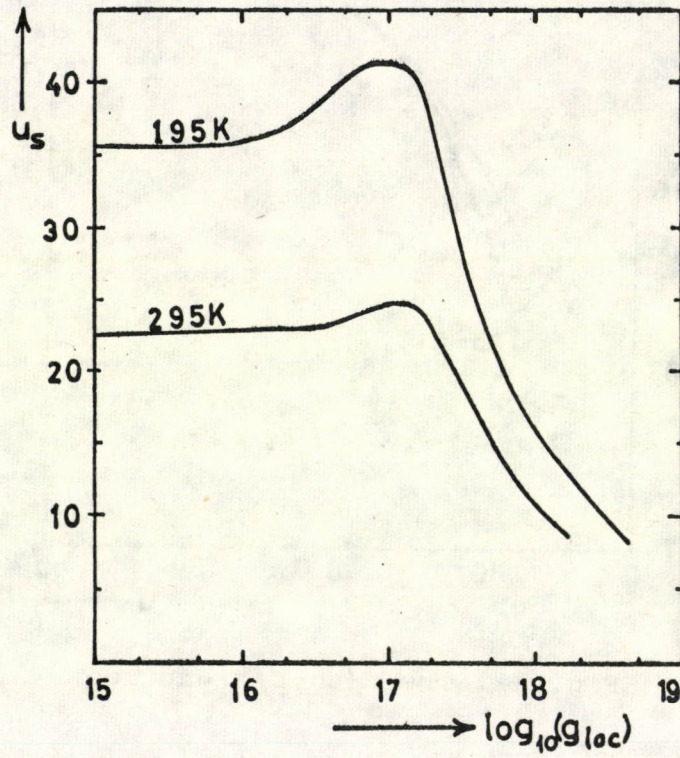
Fig. 11. The maximum values of u_s vs. g_{LOC} for the domains in Figs. 5-6 where the method of logarithmic slope works
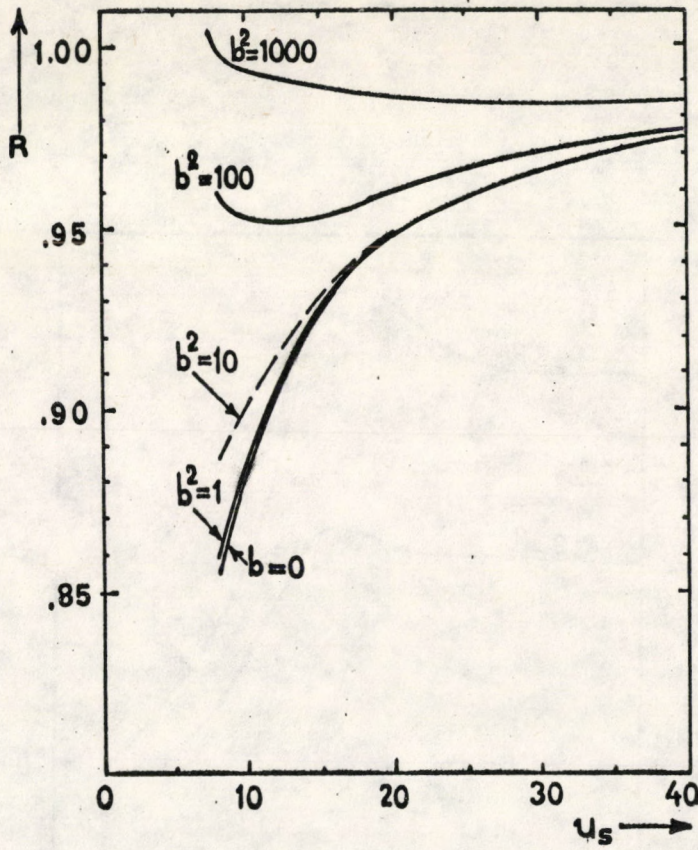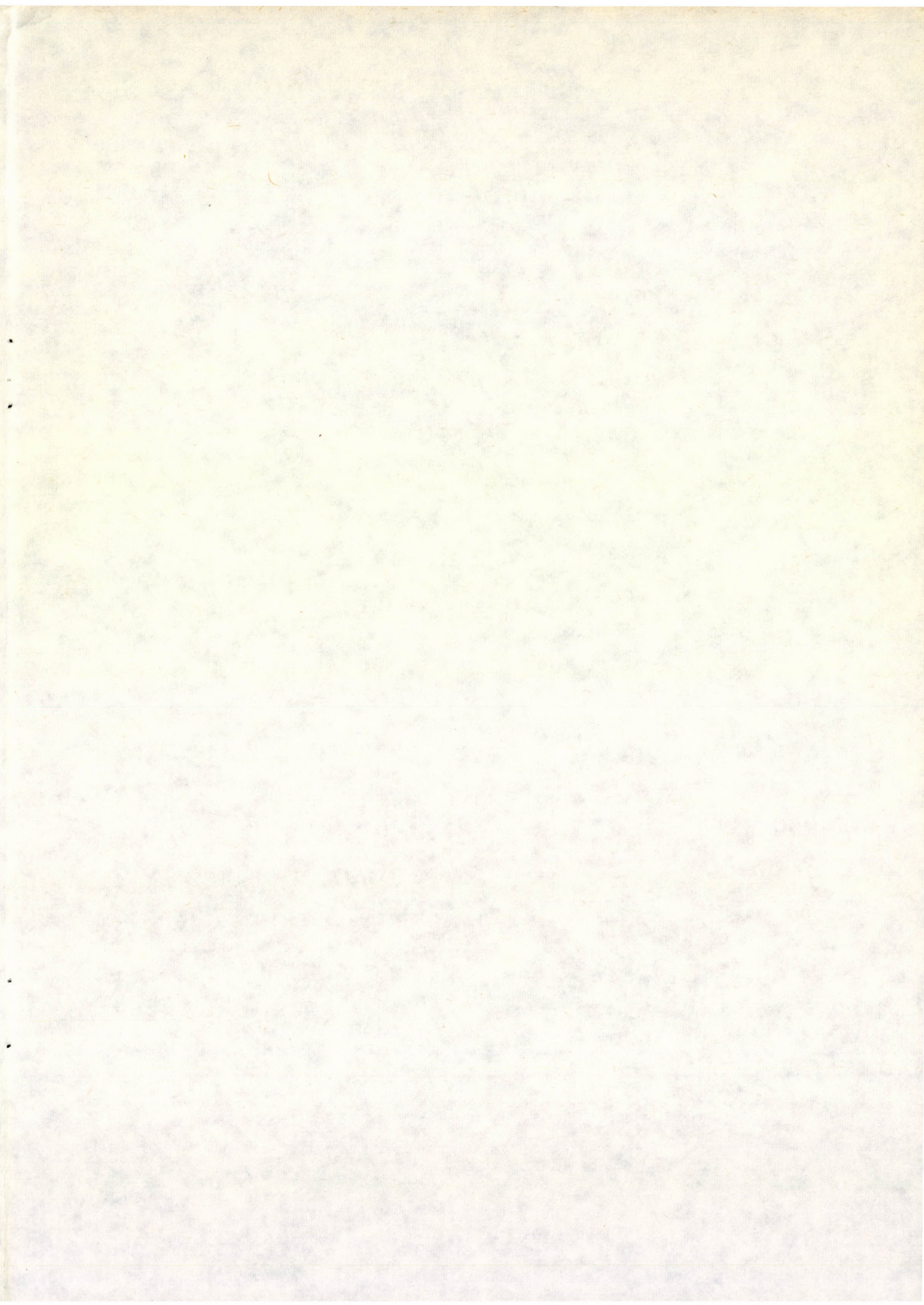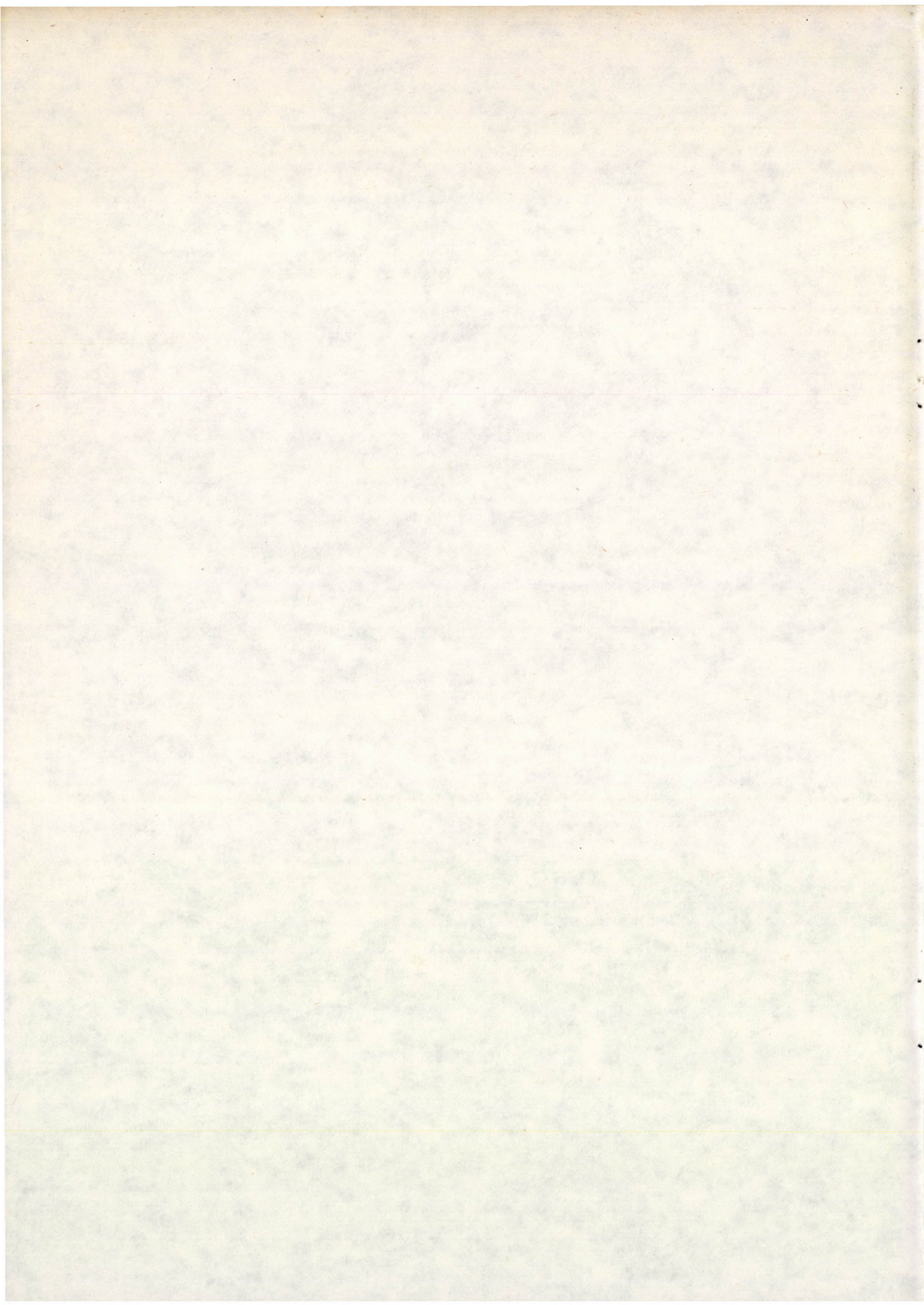
Fig. 12. The $R(u_s, b)$ function

Fig. 13. The $f(z)$ function